Electronic Supporting information:

Evaluation of Molecular Poisoning Phenomenon of W Sites in Microporous Materials by Synchrotron X-ray Powder Diffraction

Lin Ye[a], Pu Zhao[a], Molly Meng-Jung Li[a], Benedict T. W. Lo[a], Chiu Tang[b] and Shik Chi Edman Tsang*[a]

Materials and Methods:

1 Materials

1.1 H-ZSM-5 pretreatment

H-ZSM-5 (Al:Si=1:19.25) was supplied from Sinopec, China. The elemental analysis of the solid samples was performed using inductively coupled plasma-atomic emission spectroscopy (P-4010/ICP-AES). The sample was calcined in air at 480 °C for 2 h with a ramp rate of 1 °C min^{-1} before use. In addition, the BET surface area of H-ZSM-5 is 330 m^2 g^{-1}.

1.2 W modified ZSM-5 sample

W/ZSM-5 was prepared by wet impregnation. Typically, 583mg ammonia metatungstate hydrate ($(NH_4)_6H_2W_{12}O_{40}\cdot xH_2O$) was dissolved in 20 mL deionized water before 5 g zeolite was added to the solution. After 1 h magnetic stirring, the dispersion was dried in an 80 ^{o}C oven overnight. The resulting powder was ground and calcined at 550 ^{o}C for 2 h in air. The heating rate was 1 ^{o}C min^{-1}.

1.3 W-carbene/ZSM-5 and cis-stilbene adsorbed W/ZSM-5 samples

W-carbene/ZSM-5 was prepared by placing W/ZSM-5 in a flowing stream of 2-butene (2% 2-butene in N_2, 1 bar) at 400 ^{o}C for 1 h. The flow rate was 50 ml min^{-1}.

The W/ZSM-5 was heated at 200 °C for 2 hours in vacuum in a round bottle, which pre-attached to a schlenk line in order to remove trace moisture before the cis-butene adsorption. The sample was then exposed to cis-stilbene vapour for 30 minutes at room temperature.

1.4 Catalytic performance evaluation

The reaction between ethene ($C_2^=$) and *trans*-2-butene (*trans*-2-$C_4^=$, $n(C_2^=)/n($*trans*-2- $C_4^=) =$ 2/1) was carried out in a stainless steel continuous flow reactor (3/8 inch ID and 15 inch length).

In a typical experiment, 2.1 g catalyst (15−20 cm length) was loaded into the reactor with quartz wool packed at both ends. The catalyst was pretreated in N_2 (16 ml min^{-1}) at 550°C for 1 h. After the reactor cooled down to the reaction temperature, the reactants, 4% $C_2^=/N_2$ and 2% *trans*-2-$C_4^=/N_2$, were introduced (105 ml min^{-1} each, WHSV = 0.27 h^{-1}, GHSV = 26−35 h^{-1}). The flow rates were controlled by Brooks mass flow controllers. The reaction temperature was controlled by a custom-made furnace. The reaction pressure was controlled by a Swagelok back pressure regulator. The products were analyzed online by a Shimadzu GC-2014 gas chromatograph equipped with a SGE BP-1 column (100% dimethyl polysiloxane, 30 m length, 0.53 mm ID, 5.0 µm film thickness) and an FID detector. The *trans*-2-butene conversion, propene selectivity, and carbon balance were calculated as follows:

$$\text{Conversion}\left(trans-2-\mathrm{C}_4^=\right)=\frac{n\left(trans-2-\mathrm{C}_4^=\text{ in feed}\right)-n(trans-2-\mathrm{C}_4^=\text{ remaining})}{n\left(trans-2-\mathrm{C}_4^=\text{ in feed}\right)}$$

$$\text{Selectivity}(\mathrm{C}_3^=)=\frac{n(\mathrm{C}_3^=)}{n(\text{all products})}$$

$$\text{Carbon balance}=\frac{n(\mathrm{C})\text{ in products}}{n(\mathrm{C})\text{ in feed}}$$

2 Laboratory characterization

2.1 Transmission electron microscopy (TEM)

The morphology and microstructure were examined by transmission electron microscopy (TEM) using a JEOL 3000F microscope. TEM specimens were prepared by pipetting 5 µl of the sample dispersion in ethanol onto holey carbon-coated copper mesh grids (400 meshes).

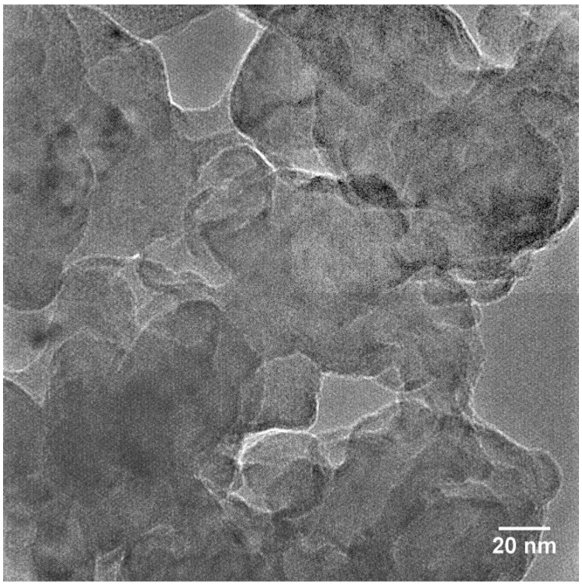

Fig. S1. TEM images of W/ZSM-5.

Figure S1 shows neither detectable WO_x clusters nor WO_3 nanoparticles, indicating WO_x are well dispersed over ZSM-5 catalyst.

2.2 Raman

Raman spectra were measured using a Horiba Jobin Yvon LabRAM HR800 spectrometer with laser excitation at 532 nm (2.33 eV). Measurements were taken with 5 s exposure. The Raman spectrometer was calibrated using a silicon standard beforehand.

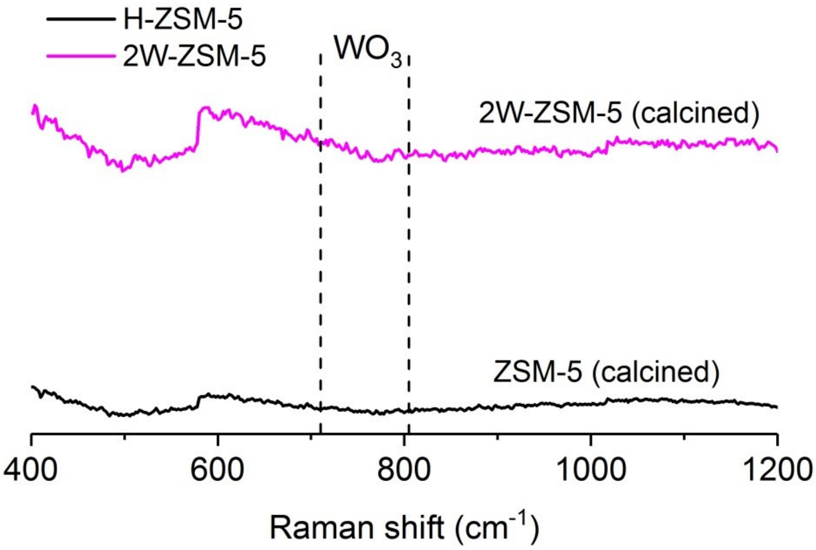

Figure S2. Raman spectra of W/ZSM-5 and H-ZSM-5

It is well-reported that Raman peaks attributable to O−W(−O) of WO_3 crystals at around 710 and 810 cm^{-1} with the assigned W-O-W vibrations in the range from 200 to 300 $cm^{-1,}$ which are not seen in W/ZSM-5. That means that there is no polymerization of monotungstate at 8 wt% W loading.

2.3 Temperature-programmed desorption of NH_3 (NH_3-TPD)

Temperature-programmed desorption of NH_3 (NH_3-TPD) was performed on a Micromeritics AutoChem II 2920 to evaluate the acidity of the catalysts. Prior to NH_3 adsorption at 100 ^{o}C, the catalysts were heated at 600 ^{o}C under N_2 (30 ml min^{-1}) for 40 min with a heating rate of 10 ^{o}C min^{-1} so that all the adsorbed and undesired species were removed from the surface. After 30 min NH_3 adsorption (10% NH_3/He, 30 ml min^{-1}), NH_3 was switched to N_2 (30 ml min^{-1}) for 30 min to remove the physisorbed NH_3. The analysis was conducted with He (50 ml min^{-1}) as the carrier gas in the temperature range of 100−600 ^{o}C with a heating rate of 10 ^{o}C min^{-1}.

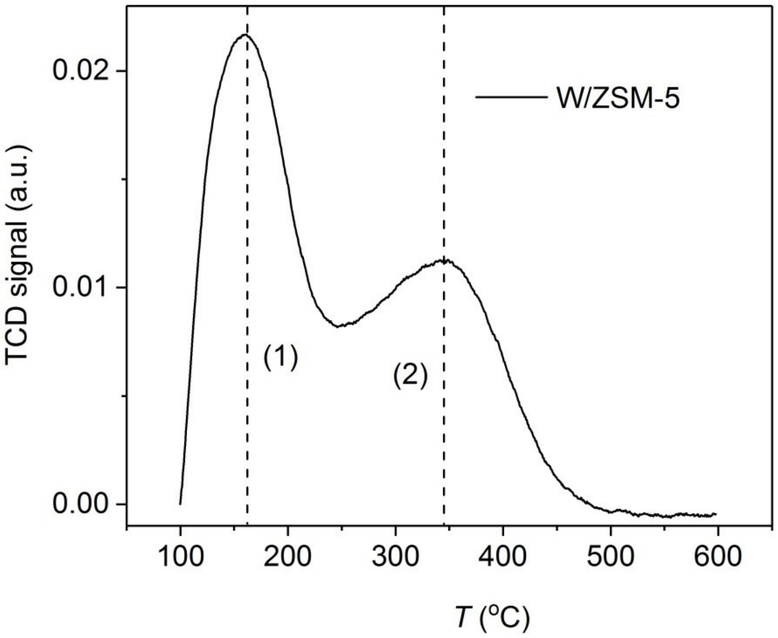

Peak	T (°C)	$n(NH_3)$ (mmol/g)
(1)	160	0.65
(2)	349	0.47

Fig. S3. NH_3-TPD of W/ZSM-5

3 Synchrotron X-ray diffraction (SXRD)

High-resolution SXRD data were collected at beamline I11, Diamond Light Source, Harwell, UK. The energy of the incident X-ray was set at 15 keV. The wavelength and the 2θ zero point were determined by fitting the diffraction data of high-quality silicon powder (SRM640c). Before data collection, W/ZSM-5 were treated under vacuum at 300 °C for 2 h. Adsorbed water should have been removed completely. W-carbene/ZSM-5 and cis-stilbene adsorbed W/ZSM-5 were prepared as described previously. All samples were loaded into borosilicate glass capillaries (0.7 mm ID) in a glove box. Glass wool was packed on top of the sample. The SXRD data were collected in a Debye-Scherrer geometry using multi-analyzer crystals (MAC) detectors in the 2θ range of 0–150° with 0.001° data binning. Each data set was collected for 1 h for good statistics.

Rietveld refinement was performed using TOPAS-Academic. ZSM-5 zeolite starting model is obtained from reference from Heo et al[1]. All SXRD peaks appear at below 2θ = 55°, thus data at 3–55° were used for Rietveld refinement. In total, there are 4186 *hkl* reflections measured within this 2θ range, of which at least 300 independent ones were observed. From a mathematical perspective, the number of variables should not exceed the number of observables. In the Rietveld refinement performed in this work, the number of varied structural parameters has not exceeded 300. Thus, the resulting crystallographic models are reliable. The background was described by a shifted Chebyschev function. A Thompson-Cox-Hastings pseudo-Voigt peak function was used to describe the shape of diffraction peaks. The scale factor and lattice parameters were allowed to vary at all times. Refined structural parameters include the fractional coordinates (x, y, z), isotropic displacement factors (B_{eq}), site occupancy factors (SOFs), the translation and rotation of the axes of the rigid bodies describing the guest molecules within the zeolite framework. The rigid bodies were described by Z-matrix. The quality of the refinement was assured by a small weighted-profile R-factor (R_{wp}), a small goodness-of-fit (GOF) factor and acceptable B_{eq} within experimental errors[2]. All the errors of the atom-atom distances were calculated using the following equation:

$$r_{error} = \sqrt{(x_{error})^2 + (y_{error})^2 + (z_{error})^2} \times r_{measure}$$

where r_{error} is the error of the measured atom-atom distance, x_{error}, y_{error}, z_{error} are the errors of the fractional coordinates (x, y, z) respectively, $r_{measure}$ is the measured atom-atom distance.

The crystallographic data and refinement details of all samples are summarized in Table S1. The atomic arrangements of these samples are presented in Tables S2-S5. They reflect the reliability of the atomic positions and angles within acceptable experimental errors to account for the experimental desorption data.

Table S1. Crystallographic data and details of W/ZSM-5 samples, W-carbene/ZSM-5 and Cis-stilbene adsorbed W/ZSM-5.

Samples	W/ZSM-5	W-carbene/ZSM-5	Cis-stilbene W/ZSM-5
Crystal system	Orthorhombic	Orthorhombic	Orthorhombic
Space group	*Pnma*	*Pnma*	*Pnma*
Chemical formula	$H_{4.74}Al_{4.74}Si_{91.26}O_{192} \cdot 2.16W$	$H_{4.74}Al_{4.74}Si_{91.26}O_{192} \cdot 2.16W$	$H_{4.74}Al_{4.74}Si_{91.26}O_{192} \cdot 2.16W$
2 θ range refinement (°)	3 – 55	3 – 55	3 – 55
Detector	Multi-analyser crystals crystals	Multi-analyser crystals	Multi-analyser crystals
Number of parameters	148	154	159
Number of hkls	4186	4186	4170
Refinement methods	Rietveld	Rietveld	Rietveld
a (Å)	20.11243(5)	20.13722(3)	20.11895(4)
b (Å)	19.93296(4)	19.94818(3)	19.92728(4)
c (Å)	13.42581(4)	13.43269(2)	13.42284(3)
V (Å^3)	5382.411(80)	5395.923(18)	5381.431(48)
R_{wp} / R_p / R_{exp} (%)	9.474/6.945/3.457	8.916/6.899/2.592	9.990/7.363/3.201
Wavelength (Å)	0.825866(2)	0.825843(2)	0.825866(2)
2θ Zero point (°)	-0.005560(2)	0.008805(2)	-0.005560(2)
Gof χ^2	2.740	3.440	3.121

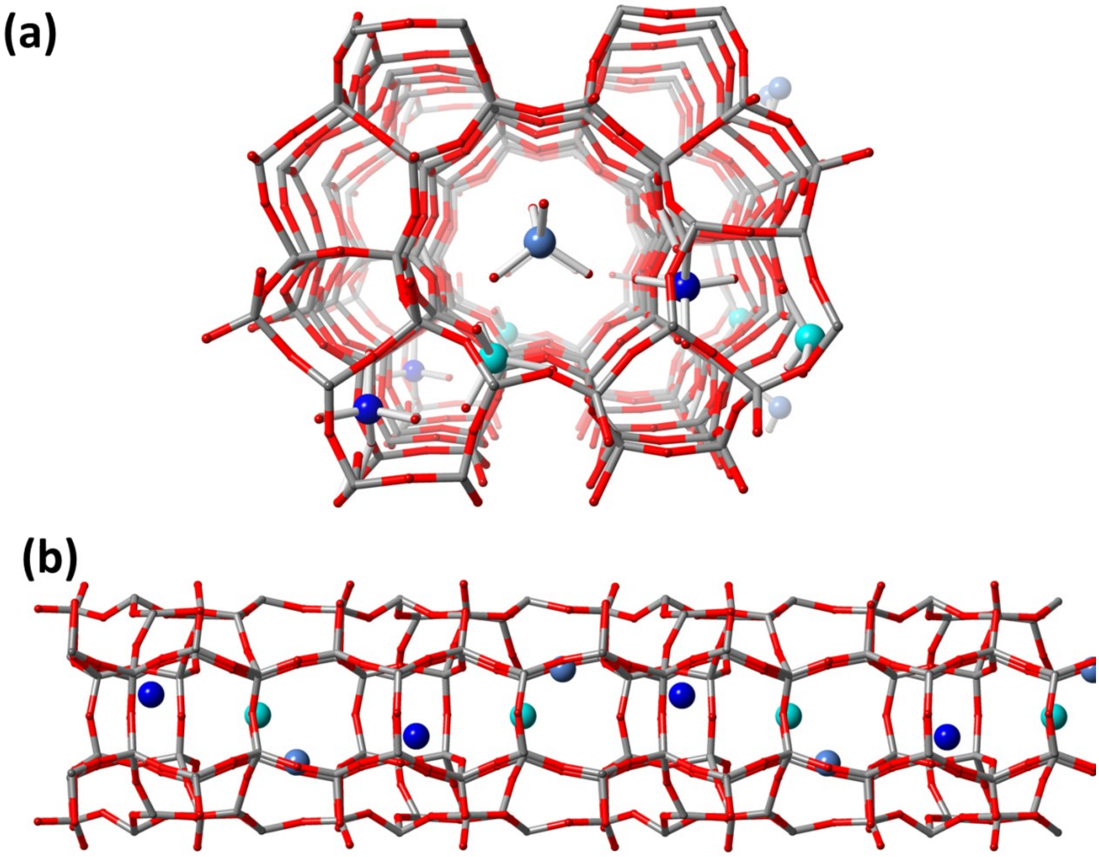

Fig. S4. The refined structure of W/ZSM-5. (a) View from the straight channel. (b) View from the sinusoidal channel. Three different W species are illustrated in different shades of blue. The oxygens of O_2=W-$(OH)_2$ are not shown in (b). The stick-ball model is used, with red = O, grey = Si, and blue = W. The symmetric W species between the mirror plane are not illustrated.

Table S2. Atomic parameters from the Rietveld refinement of W/ZSM-5 at room temperature.

Species	Atom	*X*	*y*	*Z*	SOF	B_{eq} (Å^2)	Wyckoff
Zeolite framework	O1	0.3680(6)	0.0645(7)	0.7534(8)	1	2.654(60)	8d
	O2	0.3122(6)	0.0583(7)	0.9213(7)	1	2.654(60)	8d
	O3	0.1947(6)	0.0546(6)	0.0205(6)	1	2.654(60)	8d
	O4	0.0999(4)	0.0553(7)	0.9147(9)	1	2.654(60)	8d
	O5	0.1107(6)	0.0616(7)	0.7227(8)	1	2.654(60)	8d
	O6	0.2492(6)	0.0586(8)	0.7552(8)	1	2.654(60)	8d
	O7	0.3754(7)	0.8412(5)	0.7729(8)	1	2.654(60)	8d
	O8	0.3075(7)	0.8389(5)	0.9361(8)	1	2.654(60)	8d
	O9	0.1916(7)	0.8420(4)	0.0193(6)	1	2.654(60)	8d
	O10	0.0792(5)	0.8518(6)	0.9097(9)	1	2.654(60)	8d
	O11	0.1191(7)	0.8432(6)	0.7536(8)	1	2.654(60)	8d
	O12	0.2429(6)	0.8540(6)	0.7429(9)	1	2.654(60)	8d
	O13	0.3131(5)	0.9440(6)	0.8141(6)	1	2.654(60)	8d
	O14	0.0773(5)	0.9587(6)	0.8137(8)	1	2.654(60)	8d
	O15	0.4230(5)	0.1368(5)	0.6174(8)	1	2.654(60)	8d
	O16	0.4035(5)	1.0029(6)	0.5671(0)	1	2.654(60)	8d
	O17	0.4032(6)	0.8685(6)	0.5874(9)	1	2.654(60)	8d
	O18	0.2075(6)	0.1193(6)	0.6254(8)	1	2.654(60)	8d
	O19	0.1897(7)	0.0009(6)	0.5888(8)	1	2.654(60)	8d
	O20	0.1935(7)	0.8788(6)	0.5874(8)	1	2.654(60)	8d
	O21	0.9905(6)	0.0479(7)	0.7873(8)	1	2.654(60)	8d
	O22	0.9972(7)	0.8512(6)	0.7955(8)	1	2.654(60)	8d
	O23	0.4120(7)	0.7500	0.6220(2)	1	2.654(60)	4c
	O24	0.1844(9)	0.7500	0.6458(1)	1	2.654(60)	4c
	O25	0.2797(8)	0.7500	0.0560(2)	1	2.654(60)	4c
	O26	0.1068(8)	0.7500	0.0521(2)	1	2.654(60)	4c
	Si1	0.4209(3)	0.0497(4)	0.6623(5)	1	1.410(27)	8d
	Si2	0.3093(4)	0.0280(3)	0.8144(5)	1	1.410(27)	8d
	Si3	0.2749(3)	0.0590(4)	0.0359(4)	1	1.410(27)	8d

	Si4	0.1171(3)	0.0639(3)	0.0196(5)	1	1.410(27)	8d
	Si5	0.0694(3)	0.0306(3)	0.8145(5)	1	1.410(27)	8d
	Si6	0.1832(3)	0.0598(3)	0.6736(5)	1	1.410(27)	8d
	Si7	0.4235(3)	0.8249(3)	0.6739(6)	1	1.410(27)	8d
	Si8	0.3050(4)	0.8714(3)	0.8125(4)	1	1.410(27)	8d
	Si9	0.2760(3)	0.8257(3)	0.0318(5)	1	1.410(27)	8d
	Si10	0.1216(3)	0.8255(3)	0.0349(5)	1	1.410(27)	8d
	Si11	0.0714(3)	0.8650(3)	0.8167(5)	1	1.410(27)	8d
	Si12	0.1869(4)	0.8261(3)	0.6796(5)	1	1.410(27)	8d
W^a species	Translate	0.7780(10)	0.2877(11)	0.6025(15)			
	Wa	0.7780	0.2877	0.6025	0.082(1)	1.6(7)	8d
	OWa1	0.791	0.364	0.535	0.082(1)	2.5	8d
	OWa2	0.842	0.228	0.572	0.082(1)	2.5	8d
	OWa3	0.781	0.306	0.742	0.082(1)	2.5	8d
	OWa4	0.693	0.252	0.568	0.082(1)	2.5	8d
W^b species	Translate	0.9231(12)	0.7492(39)	0.2272(17)			
	Wb	0.9231	0.7492	0.2272	0.089(2)	11.0(9)	8d
	OWb1	0.900	0.828	0.279	0.089(2)	16.5	8d
	OWb2	0.883	0.738	0.109	0.089(2)	16.5	8d
	OWb3	1.017	0.75	0.210	0.089(2)	16.5	8d
	OWb4	0.900	0.679	0.315	0.089(2)	16.5	8d
W^c species	Translate	1.0032(14)	0.3370(11)	0.4994(15)			
	Wc	1.0032	0.3370	0.4994	0.090(2)	4.1(8)	8d
	OWc1	1.074	0.339	0.580	0.090(2)	6.1	8d
	OWc2	0.929	0.326	0.572	0.090(2)	6.1	8d
	OWc3	0.997	0.419	0.427	0.090(2)	6.1	8d
	OWc4	1.012	0.264	0.408	0.090(2)	6.1	8d

All the T-sites (T=Al, Si) of ZSM-5 were refined using the same B_{eq} parameter.

All the O-sites of ZSM-5 were refined using the same B_{eq} parameter.

The values for the O-sites of W species were refined using the same SOF and 1.5 times of the B_{eq} for the coordinated W-sites.

Table S3. R-factors of W-carbene/ZSM-5 that C-C added one by one and W-carbene rigid body.

Samples	Rietveld R_{wp} / R_p / R_{exp} / χ^2
W/ZSM-5· 1C-C	8.909/6.899/2.592/3.44
W/ZSM-5· 2C-C	8.887/6.875/2.592/3.43
W/ZSM-5· 3C-C	8.768/6.763/2.592/3.38
W/ZSM-5· W=C rigid body	8.916/6.899/2.592/3.43

Table S4. Atomic parameters from the Rietveld refinement of W-carbene/ZSM-5 at room temperature.

Species	Atom	*X*	*y*	*Z*	SOF	B_{eq} (Å^2)	Wyckoff
Zeolite framework	O1	0.3680(4)	0.0645(4)	0.7534(5)	1	2.385(58)	8d
	O2	0.3122(4)	0.0583(4)	0.9213(5)	1	2.385(58)	8d
	O3	0.1947(4)	0.0546(4)	0.0205(4)	1	2.385(58)	8d
	O4	0.0999(3)	0.0553(4)	0.9147(6)	1	2.385(58)	8d
	O5	0.1107(4)	0.0616(4)	0.7227(5)	1	2.385(58)	8d
	O6	0.2492(4)	0.0586(5)	0.7552(5)	1	2.385(58)	8d
	O7	0.3754(4)	0.8412(3)	0.7729(5)	1	2.385(58)	8d
	O8	0.3075(4)	0.8389(3)	0.9361(5)	1	2.385(58)	8d
	O9	0.1916(4)	0.8420(3)	0.0193(4)	1	2.385(58)	8d
	O10	0.0792(3)	0.8518(4)	0.9097(6)	1	2.385(58)	8d
	O11	0.1191(4)	0.8432(3)	0.7536(5)	1	2.385(58)	8d
	O12	0.2429(4)	0.8540(4)	0.7429(6)	1	2.385(58)	8d
	O13	0.3131(3)	0.9440(4)	0.8141(4)	1	2.385(58)	8d
	O14	0.0773(3)	0.9587(4)	0.8137(5)	1	2.385(58)	8d
	O15	0.4230(3)	0.1368(3)	0.6174(5)	1	2.385(58)	8d
	O16	0.4035(4)	1.0029(4)	0.5671(6)	1	2.385(58)	8d
	O17	0.4032(4)	0.8685(4)	0.5874(6)	1	2.385(58)	8d
	O18	0.2075(4)	0.1193(3)	0.6254(5)	1	2.385(58)	8d

	O19	0.1897(5)	0.0009(4)	0.5888(5)	1	2.385(58)	8d
	O20	0.1935(5)	0.8788(3)	0.5874(5)	1	2.385(58)	8d
	O21	0.9905(4)	0.0479(5)	0.7873(5)	1	2.385(58)	8d
	O22	0.9972(4)	0.8512(4)	0.7955(5)	1	2.385(58)	8d
	O23	0.4120(5)	0.7500	0.6220(8)	1	2.385(58)	4c
	O24	0.1844(6)	0.7500	0.6458(7)	1	2.385(58)	4c
	O25	0.2797(5)	0.7500	0.0560(8)	1	2.385(58)	4c
	O26	0.1068(5)	0.7500	0.0521(8)	1	2.385(58)	4c
	Si1	0.4209(2)	0.0497(2)	0.6623(3)	1	1.372(22)	8d
	Si2	0.3093(3)	0.0280(2)	0.8144(3)	1	1.372(22)	8d
	Si3	0.2749(2)	0.0590(2)	0.0359(3)	1	1.372(22)	8d
	Si4	0.1171(2)	0.0639(2)	0.0196(3)	1	1.372(22)	8d
	Si5	0.0694(2)	0.0306(2)	0.8145(4)	1	1.372(22)	8d
	Si6	0.1832(2)	0.0598(2)	0.6736(3)	1	1.372(22)	8d
	Si7	0.4235(2)	0.8249(2)	0.6739(4)	1	1.372(22)	8d
	Si8	0.3050(2)	0.8714(2)	0.8125(3)	1	1.372(22)	8d
	Si9	0.2760(2)	0.8257(2)	0.0318(3)	1	1.372(22)	8d
	Si10	0.1216(2)	0.8255(2)	0.0349(3)	1	1.372(22)	8d
	Si11	0.0714(2)	0.8650(2)	0.8167(3)	1	1.372(22)	8d
	Si12	0.1869(2)	0.8261(2)	0.6796(3)	1	1.372(22)	8d
W^a species	Translate	0.7780(10)	0.2877(11)	0.6025(15)			
	Wa	0.7780	0.2877	0.6025	0.082(1)	1.6(7)	8d
	OWa1	0.791	0.364	0.535	0.082(1)	2.5	8d
	OWa2	0.842	0.228	0.572	0.082(1)	2.5	8d
	OWa3	0.781	0.306	0.742	0.082(1)	2.5	8d
	CWa1	0.856	0.230	0.553	0.082(1)	2.5	8d
	CWa2	0.931	0.220	0.559	0.082(1)	2.5	
W^b species	Translate	0.9231(12)	0.7492(39)	0.2272(17)			
	Wb	0.9231	0.7492	0.2272	0.089(2)	11.0(9)	8d
	OWb1	0.900	0.828	0.279	0.089(2)	16.5	8d

	OWb2	0.883	0.738	0.109	0.089(2)	16.5	8d
	OWb3	1.017	0.75	0.210	0.089(2)	16.5	8d
	CWb1	0.978	0.689	0.313	0.089(2)	16.5	8d
	CWb2	0.975	0.697	0.427	0.089(2)	16.5	
W^c species	Translate	1.0032(14)	0.3370(11)	0.4994(15)			
	Wc	1.0032	0.3370	0.4994	0.090(2)	4.1(8)	8d
	OWc1	1.074	0.339	0.580	0.090(2)	6.1	8d
	OWc2	0.929	0.326	0.572	0.090(2)	6.1	8d
	OWc3	0.997	0.419	0.427	0.090(2)	6.1	8d
	CWc1	0.980	0.427	0.445	0.090(2)	6.1	8d
	CWc2	1.000	0.489	0.382	0.090(2)	6.1	

All the T-sites (T=Al, Si) of ZSM-5 were refined using the same B_{eq} parameter.

All the O-sites of ZSM-5 were refined using the same B_{eq} parameter.

The values for the O-sites and C-sites of W species were refined using the same SOF and 1.5 times of the B_{eq} for the coordinated W-sites.

Table S5. Atomic parameters from the Rietveld refinement of cis-stilbene adsorbed W/ZSM-5 at room temperature.

Species	Atom	*X*	*y*	*Z*	SOF	B_{eq} (Å^2)	Wyckoff
Zeolite framework	O1	0.3683(5)	0.0563(6)	0.7613(7)	1	2.094(40)	8d
	O2	0.3055(6)	0.0687(4)	0.9158(6)	1	2.094(40)	8d
	O3	0.2009(5)	0.0541(5)	0.0238(5)	1	2.094(40)	8d
	O4	0.0973(4)	0.0561(6)	0.9265(7)	1	2.094(40)	8d
	O5	0.1131(5)	0.0594(6)	0.7185(7)	1	2.094(40)	8d
	O6	0.2549(5)	0.0582(7)	0.7569(7)	1	2.094(40)	8d
	O7	0.3746(5)	0.8444(5)	0.7827(7)	1	2.094(40)	8d
	O8	0.3145(5)	0.8407(4)	0.9354(6)	1	2.094(40)	8d
	O9	0.1901(5)	0.8464(4)	0.0178(5)	1	2.094(40)	8d
	O10	0.0853(5)	0.8507(5)	0.9000(7)	1	2.094(40)	8d
	O11	0.1233(5)	0.8459(5)	0.7533(7)	1	2.094(40)	8d
	O12	0.2416(5)	0.8439(6)	0.7435(7)	1	2.094(40)	8d
	O13	0.3105(5)	0.9415(4)	0.8186(5)	1	2.094(40)	8d
	O14	0.0794(4)	0.9620(4)	0.8168(7)	1	2.094(40)	8d

	O15	0.4210(5)	0.1357(4)	0.6247(7)	1	2.094(40)	8d
	O16	0.4083(5)	1.0004(5)	0.5670(7)	1	2.094(40)	8d
	O17	0.4112(5)	0.8681(5)	0.5864(8)	1	2.094(40)	8d
	O18	0.1852(5)	0.1188(4)	0.6162(7)	1	2.094(40)	8d
	O19	0.1979(6)	-0.0005(5)	0.6054(7)	1	2.094(40)	8d
	O20	0.2053(6)	0.8732(5)	0.5789(7)	1	2.094(40)	8d
	O21	0.9954(5)	0.0429(6)	0.7781(6)	1	2.094(40)	8d
	O22	0.9914(5)	0.8476(5)	0.7923(7)	1	2.094(40)	8d
	O23	0.4148(7)	0.7500	0.6254(1)	1	2.094(40)	4c
	O24	0.2073(7)	0.7500	0.6479(9)	1	2.094(40)	4c
	O25	0.2881(7)	0.7500	0.0542(9)	1	2.094(40)	4c
	O26	0.1156(7)	0.7500	0.0614(9)	1	2.094(40)	4c
	Si1	0.4217(3)	0.0503(3)	0.6669(4)	1	1.253(19)	8d
	Si2	0.3083(4)	0.0291(2)	0.8169(4)	1	1.253(19)	8d
	Si3	0.2767(2)	0.0593(3)	0.0326(4)	1	1.253(19)	8d
	Si4	0.1163(2)	0.0650(3)	0.0275(4)	1	1.253(19)	8d
	Si5	0.0711(3)	0.0321(3)	0.8145(5)	1	1.253(19)	8d
	Si6	0.1866(3)	0.0577(3)	0.6762(4)	1	1.253(19)	8d
	Si7	0.4244(3)	0.8261(3)	0.6738(5)	1	1.253(19)	8d
	Si8	0.3087(3)	0.8713(2)	0.8170(4)	1	1.253(19)	8d
	Si9	0.2769(3)	0.8273(2)	0.0313(4)	1	1.253(19)	8d
	Si10	0.1238(3)	0.8278(3)	0.0354(4)	1	1.253(19)	8d
	Si11	0.0702(3)	0.8661(3)	0.8176(5)	1	1.253(19)	8d
	Si12	0.1888(3)	0.8250(2)	0.6770(5)	1	1.253(19)	8d
W^a species	Translate	0.7780(10)	0.2877(11)	0.6025(15)			
	Wa	0.7780	0.2877	0.6025	0.082(1)	1.8(4)	8d
	OWa1	0.791	0.364	0.535	0.082(1)	2.7	8d
	OWa2	0.842	0.228	0.572	0.082(1)	2.7	8d
	OWa3	0.781	0.306	0.742	0.082(1)	2.7	8d
	OWa4	0.693	0.252	0.568	0.082(1)	2.7	8d

W^b species	Translate	0.9231(12)	0.7492(39)	0.2272(17)			
	Wb	0.9231	0.7492	0.2272	0.089(2)	5.1(5)(9)	8d
	OWb1	0.900	0.828	0.279	0.089(2)	7.7	8d
	OWb2	0.883	0.738	0.109	0.089(2)	7.7	8d
	OWb3	1.017	0.75	0.210	0.089(2)	7.7	8d
	OWb4	0.900	0.679	0.315	0.089(2)	7.7	8d
W^c species	Translate	1.0032(14)	0.3370(11)	0.4994(15)			
	Wc	1.0032	0.3370	0.4994	0.090(2)	8.1(6)	8d
	OWc1	1.074	0.339	0.580	0.090(2)	12.1	8d
	OWc2	0.929	0.326	0.572	0.090(2)	12.1	8d
	OWc3	0.997	0.419	0.427	0.090(2)	12.1	8d
	OWc4	1.012	0.264	0.408	0.090(2)	12.1	8d
Cis-stilbene	C1	0.053	0.210	-0.236	0.664(3)	19.9(8)	8d
	C2	0.065	0.195	-0.134	0.664(3)	19.9(8)	8d
	C3	0.114	0.233	-0.081	0.664(3)	19.9(8)	8d
	C4	0.150	0.285	-0.130	0.664(3)	19.9(8)	8d
	C5	0.137	0.299	-0.232	0.664(3)	19.9(8)	8d
	C6	0.089	0.262	-0.285	0.664(3)	19.9(8)	8d
	C7	0.076	0.277	-0.393	0.664(3)	19.9(8)	8d
	C8	0.040	0.245	-0.462	0.664(3)	19.9(8)	8d
	C9	0.020	0.172	-0.473	0.664(3)	19.9(8)	8d
	C10	-0.026	0.153	-0.547	0.664(3)	19.9(8)	8d
	C11	-0.044	0.085	-0.558	0.664(3)	19.9(8)	8d
	C12	-0.014	0.035	-0.497	0.664(3)	19.9(8)	8d
	C13	0.034	0.054	-0.427	0.664(3)	19.9(8)	8d
	C14	0.052	0.122	-0.415	0.664(3)	19.9(8)	8d

All the T-sites (T=Al, Si) of ZSM-5 were refined using the same B_{eq} parameter.

All the O-sites of ZSM-5 were refined using the same B_{eq} parameter.

The values for the O-sites of W species were refined using the same SOF and 1.5 times of the B_{eq} for the coordinated W-sites.

The values fot the C-sites of cis-stilbene were refined using the same SOF and B_{eq}.

4 Synchrotron X-ray absorption spectroscopy (EXAFS)

Local structures surrounding W atoms in W/ZSM-5 was probed by analyzing their k3-weighted W L3-edge extended X-ray absorption fine structures (EXAFS) collected at beamline B18, Diamond Light Source, Harwell, UK. The energy resolution (ΔE/E) for the incident X-ray photons was estimated to be 2×10^{-4}. Fluorescence mode was used. To ascertain the reproducibility of the experimental data, at least two data sets were collected and compared for each sample. W metal was used as a reference to avoid energy shift of the measured EXAFS spectra. Data analysis was performed using IFEFFIT 1 with Horae packages 2 (Athena and Artemis). The amplitude parameter was set as a fixed input parameter to allow the refinement of the coordination number of W. It was obtained from the analysis of the EXAFS data of W metal. In this work, the first shell data analyses were performed under the assumption of single scattering with the errors estimated by an R-factor.

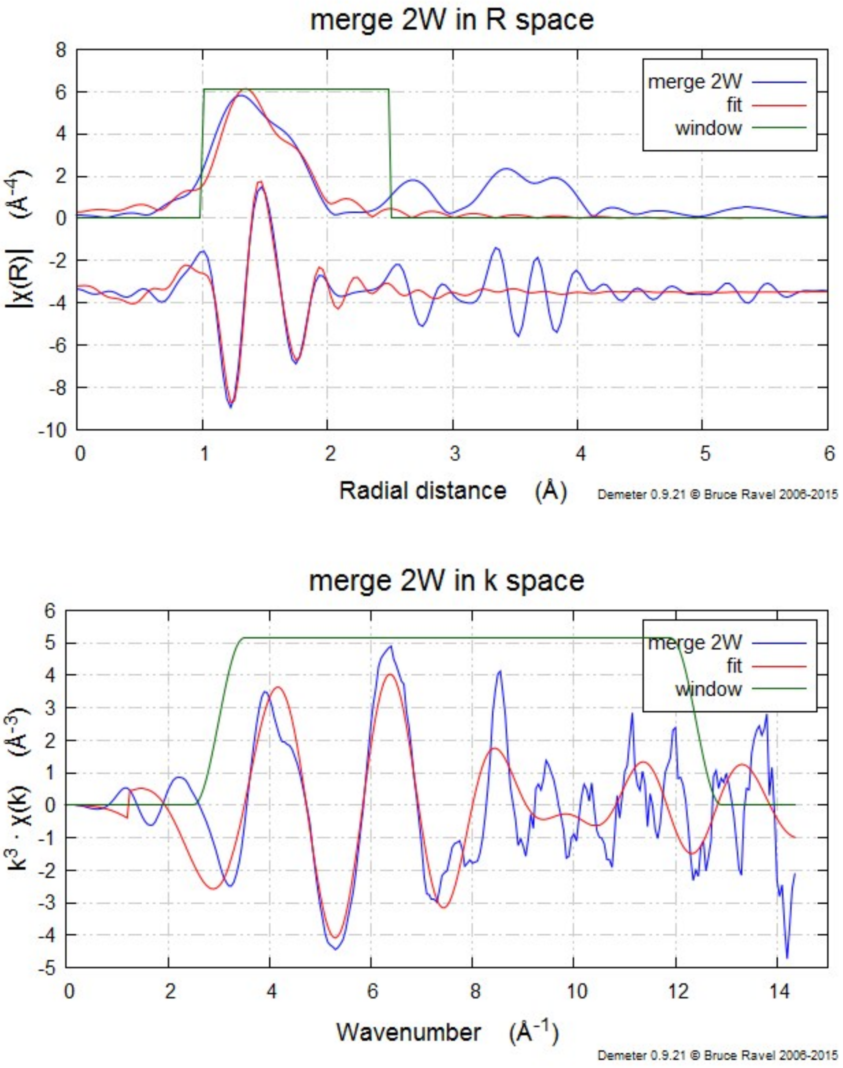

Fig. S5. (a) Fourier-transformed and k^3-weighted W L_3-edge EXAFS in *R* space of W/ZSM-5. (b) k^3-weighted W L_3-edge EXAFS of W/ZSM-5.

5 Catalytic performance of the W/ZSM-5 in olefin metathesis reaction

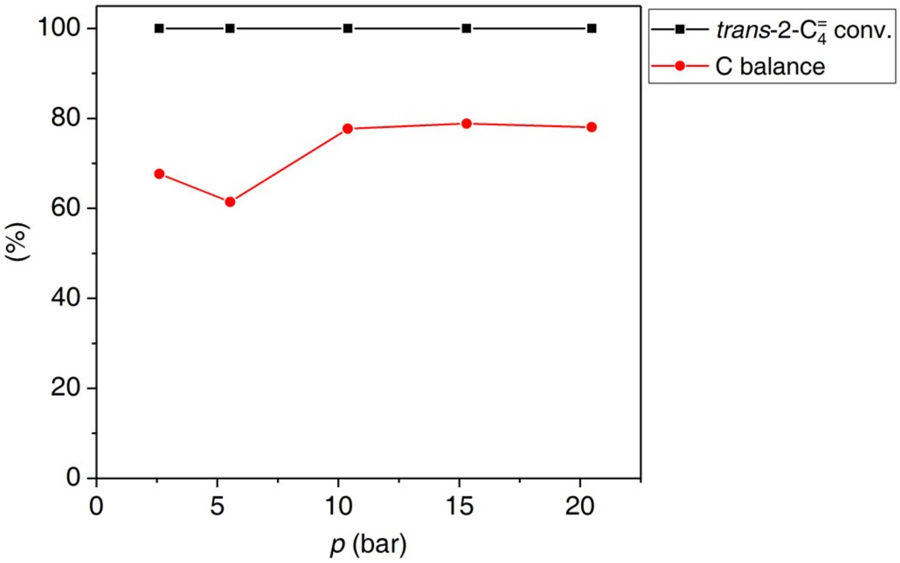

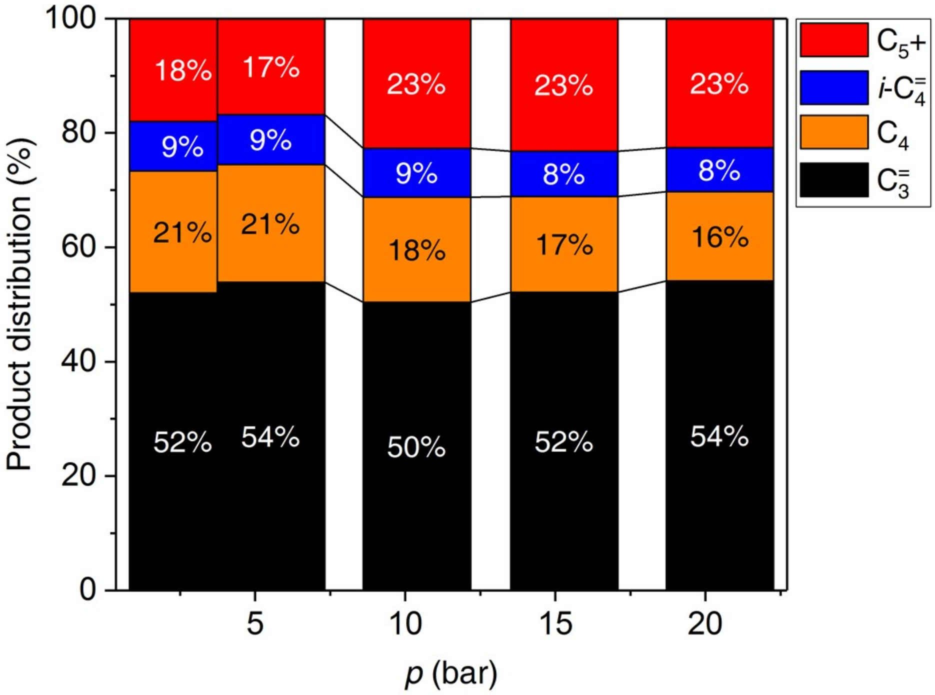

Fig. S6. Catalytic performance of W/ZSM-5 at $T = 400^{o}$C, P =1−20 bar and WHSV = 0.27 h^{-1}.

W/ZSM-5 catalyzes the conversion of trans-2-butene and ethylene to propene with the propene selectivity of 54% by metathesis along with acid catalyzed isomerization to iso-butene, cracking to n-butane and aromatization to C5^{+} at steady state. The carbon balance reaches 100% by adding up the gaseous products (67%) with carbonaceous products (33%, evaluated by thermal gravimetric analysis) at 2.26 bar.

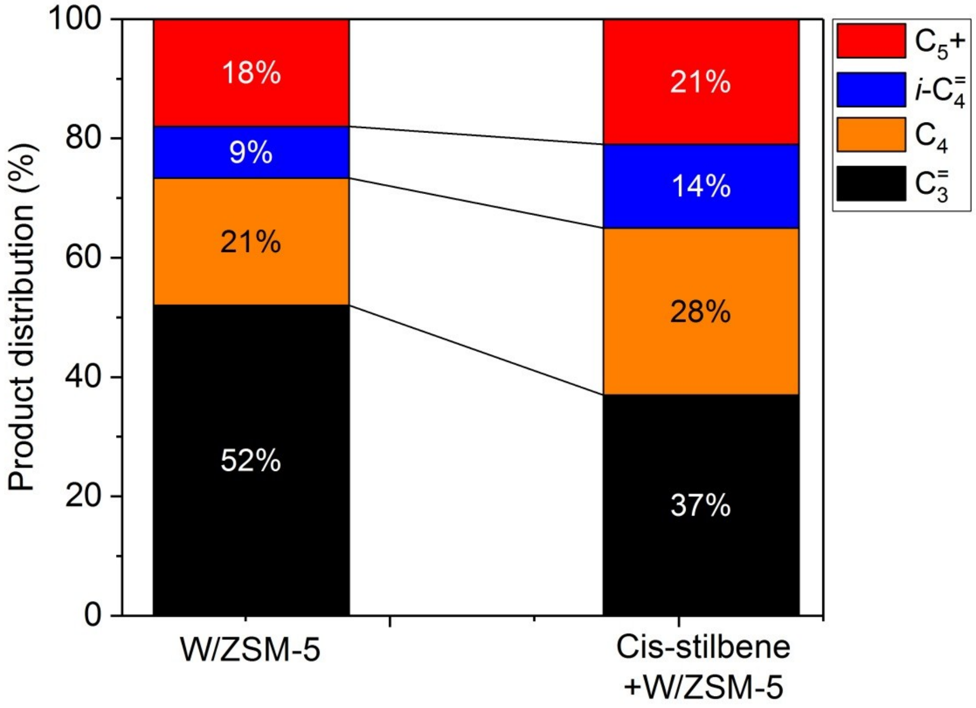

Fig. S7. Comparison of the catalytic performance of W/ZSM-5 with or without blending cis-stilbene at $T = 400^oC$, $P = 2.26$ bar and WHSV = 0.27 h^{-1}.

W/ZSM-5 catalyzes the total conversion of trans-2-butene and ethylene to propene with the propene selectivity of 52% at steady state. The carbon balance reaches 100% by adding up gaseous products (67%) with carbonaceous products (33%, evaluated by thermal gravimetric analysis). After blending the olefin substrates with trace of cis-stilbene vapor, the propene selectivity rapidly decreases and stabilizes by 1/3 of the original value to 37%. The carbon balance reaches 100% by adding up the gaseous products (66%) with carbonaceous products (34%) which appear to remain the same values in W/ZSM-5 without cis stilbene treatment. The observation for 1/3 value of the propene yield (deactivation) attenuated is consistent with the molecular poisoning phenomenon. That corresponds to 1/3 of the W species located in large cross channels region captured by the cis-stilbene instead of the cause by the initial carbonaceous deposition.

Other possible deactivation routes:

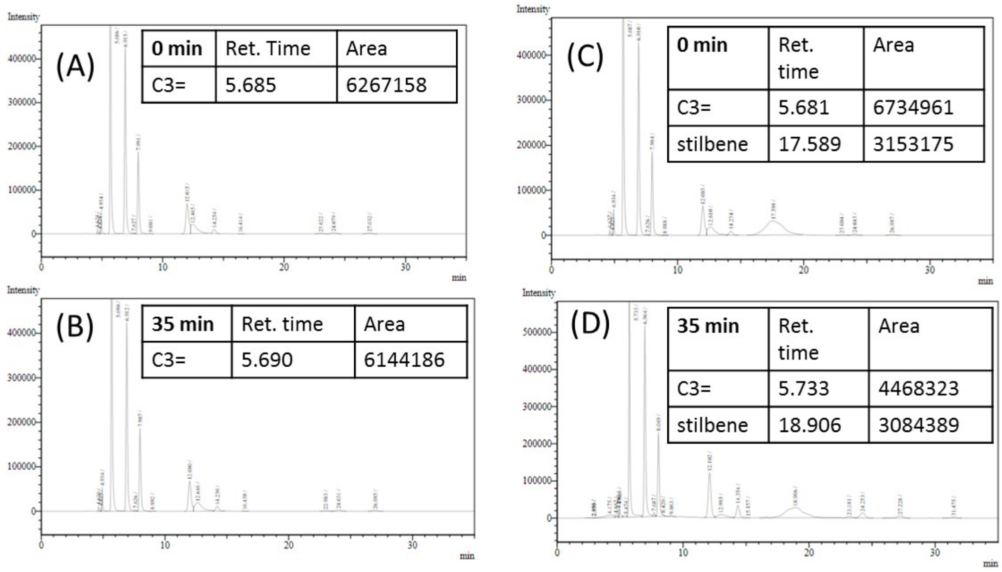

0 min	Ret. Time	Area
C3=	5.685	6267158

35 min	Ret. time	Area
C3=	5.690	6144186

0 min	Ret. time	Area
C3=	5.681	6734961
stilbene	17.589	3153175

35 min	Ret. time	Area
C3=	5.733	4468323
stilbene	18.906	3084389

Fig. S8. Comparison of the catalytic performance (GC analysis) of W/ZSM-5 without ((A) and (B)) or with ((C) and (D)) blending cis-stilbene at $T = 400^{o}$C, $P = 2.26$ bar and WHSV = 0.27 h^{-1}.

Deactivation by coke formation

We note that the formation of coke (~33%) may also led to the deactivation of the catalyst, which will complicate the above analysis. It is well accepted that carbonaceous deposition (or so called cokes) is progressively made when alkene(s) is in contact with acid sites of zeolite (oligomers and polymerisation). From the product analysis after the reaction was reaching steady state (10h, see Fig. S6 and Fig. S7), we observed the deactivation to the 2/3 of the original activity when stilbene was allowed to pass with the C_2=/C_4= mixture (Fig. S7). As a result, the deactivation could be due to stilbene or coke formation or both.

Here, we analyse the product concentration in the first 35 mins under the C_2=/C_4= with stilbene whereby the coke formation is relatively less important. As seen from Fig. S8 (A) and (B), the peak area of C_3 product from our gas chromatography does not seem to alter, which indicates that the activity of W/ZSM-5 is maintained at this initial period with no observable effect from coke formation. However, in the same experiment but this time the substrates are blended with stilbene, the peak area of C_3= is dramatically decreased (activity drops) to the 2/3 of the original activity of no blended stilbene. Clearly, stilbene is the main cause for the observed deactivation. Notice that the stilbene concentration does not change at all during this period of time (see Fig. S8 (C) and (D)), indicating that only a small amount is instantaneously needed to poison the W^c (cross channel) species for the deactivation. It is therefore unlikely to be the substrate for the continuous coke deposition. Combined the SXRD analysis, we believe that the extent of 1/3 deactivation can be mainly attributed to the cis-stilbene poisoning to the W^c (cross channel) species that also matches with the 1/3 of the total W species used.

Deactivation caused by cis-stilbene reactions

We considered the possibility whether cis-stilbene may have reacted with ethylene to form styrene, which either desorbed or polymerized. Thus, the deactivation may be complicated especially at high reaction temperature. However, during the testing, we did not detect styrene or any oligomer products. As seen from the Fig. S8, the peak area of stilbene also remains constant indicating that it does not seem to involve in any catalytic chemical reaction.

As stated in the introduction, stilbene molecule is one of the well-known compounds as a catalytic poison for metathesis reaction. Since the formation of 'W-carbene' from the W=O groups of $[(O)_2{=}W\text{-}(O)_2]^{2-}$ precursor is the crucial step to initiate the metallacyclobutane catalytic cycle (Scheme 1 in the manuscript). However, cis-stilbene can simultaneously block two of the W=O groups of $[(O)_2{=}W\text{-}(O)_2]^{2-}$ (see the sketch below), which totally inhibits any further metathesis reaction. From SXRD, we observed that the selective blocking of the W (cross channel) by the stilbene molecule.

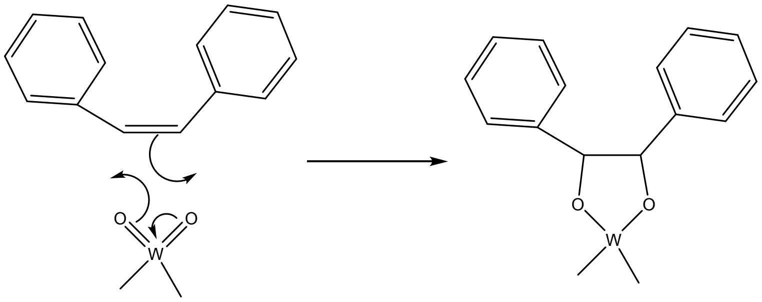

The cis-stilbene may be transformed to trans-stilbene particularly at high temperature. Despite the possible transformation, the large dynamic size of trans-stilbene (11.30 × 4.32 Å) is still substantially larger than the dimensions of the sinusoidal channel (around 5 Å), where the other two W (W^a and W^b) species are located. On the other hand, the smaller dynamic sizes of butene (4.6 × 3.1 Å) and ethene (2.4 × 1.9 Å) can allow themselves to diffuse into the sinusoidal channel to gain access to the W^a and W^b for catalysis. By refining the structure of W/ZSM-5 with stilbene, the stilbene molecule after annealing simulation converges around the W^c species in the cross channel region rather than those of W^a and W^b in the sinusoidal channel. As a result, we conclude that the stilbene only block the W^c (cross channel) species to lead to the observed deactivation as shown in the above sketch.

6 W environments in ZSM-5

We are interested whether some of W species exist to give W-W-bonding, W dimers or clusters in the ZSM-5. As mentioned in the materials synthesis section, ammonium metatungstate hydrate ($(NH_4)_6H_2W_{12}O_{40}\cdot xH_2O$) was used as the chemical precursor in this work. During impregnation and calcination but without reduction, a majority of W species still appeared to be in the form of tungstate $[(O)_2{=}W\text{-}(O)_2]^{2-}$ under the conditions (in air) according to our SXRD and EXAFS data. Thus, it is unlikely that the majority of the $[(O)_2{=}W\text{-}(O)_2]^{2-}$ can somehow be reduced to metallic W or forming W-W-bonding. In general, Raman bands of 715 and 806 cm^{-1} are attributed to WO_3 nanoparticle with the assigned W-O-W vibrations in the range from 200 to 300 cm^{-1}. However, those peaks were not shown in our Raman characterization (Fig. S2), which indicates the majority of W species are isolated from their neighbours in consistent with the SXRD and EXAFS data.

Since we only fitted the first coordination shell of W from our EXAFS data of higher accuracy, we are unsure whether the discrepancies between experimental data with fitted data of longer distances of around 0.27nm and 0.35nm were due to W-W bonding (Fig. S5). We cannot discount the fact that there may have small contributions of multiple bonding in the minor W species although the experimental errors to fit these longer distances are high.

Nevertheless, the majority of W species appear to have been anchored on ZSM-5 in isolation. We wondered how it is immobilised in the internal surface of ZSM-5. Noticeably, we have recently elucidated W in USY with the anchored W structure akin to that of ZSM-5. From the SXRD and DFT calculation[3], W species interact with the acid site on the channel wall through hydrogen bonding and the calculated adsorption energy is around -141 kJ mol^{-1}. Therefore, the anchored W species is rather stable under the reaction condition.

We had made an assumption that the three W species in the ZSM-5 showed equivalent activity. This was based on our SXRD result, which showed that all the three W species were structurally identical in the same chemical bonding environment. The only difference was that W^c species was in the larger cross channel region and the other two W species (W^a and W^b) were in smaller sinusoidal cavity of ZSM-5. The substrate molecules (butene/ethane) being smaller sizes compared to these channel openings, they should react with the three W species in the same manner, giving equivalent activity. After introducing trace amount of cis-stilbene, we indeed observed the propene yield rapidly attenuated by 1/3, which correlated to the poisoned W^c species (1/3 of the W species) located in large cross channels region by the cis-stilbene.

We carried out EXAFS analysis of deactivated W/ZSM-5 which we think is very important to understand its chemical environment of W. It is however, we encountered some issues in the EXAFS analysis of this deactivated sample. It appeared that the stilbene molecule adsorption on the W species had altered their chemical environment rendering the EXAFS fitting against our ideal model rather poor. At this stage, we therefore mainly used SXRD with Rietveld refinement to address the structures of W species in ZSM-5 in the deactivated sample. We are in the process of controlling the stilbene concentration and investigating some new fitting methods for the EXAFS data acquisition of the deactivated sample to further support this study.

7 Generic nature of SXRD and Rietveld refinement method

It is interesting to ask whether this SXRD/refinement method is also useful for identifying the other metals and complexes inside the channels of zeolites. So far, we have successfully elucidated the W in USY zeolite[3]; the location of the extra-framework Al in the cavity of zeolite Y, which gives the explanation on the enhancement of acidic strength in dealuminated zeolite Y[4]. Also, the Zn-OH active site structure in Zn/ZSM-5 catalyst for decarboxylation in GVL has been interrogated using SXRD[5]. Notably, in combination with NMR, ICP, TGA, this SXRD method is very sensitive to the changes of the electron density of periodic scattering atoms hence the structures of their metal, metal complex or even gas molecule adsorptions could be in principle identified.

1. N. H. Heo, C. W. Kim, H. J. Kwon, G. H. Kim, S. H. Kim, S. B. Hong and K. Seff, J. Phys. Chem. C, 113, (2009), 19937-19956.
2. B. H. Toby, Powder Diffraction, 21, (2006), 67-70.
3. P. Zhao, L. Ye, Z. Sun, B. T.W. Lo, H. Woodcock, C. Huang, C. Tang, A. I. Kirkland, D. Mei, and S. C. E. Tsang. J. Am. Chem. Soc., DOI: 10.1021/jacs.8b03012, 2018.
4. L. Ye, I. Teixeira, B. T. W. Lo, P. Zhao, S. C. E. Tsang, Chem. Commun. *53*, (2017), 9725-9728.
5. L. Ye, Q. Song, B. T. W. Lo, J. L. Zheng, D. J. Kong, C. A. Murray, C. C. Tang, S. C. E. Tsang, Angew. Chem.-Int. Edit. 56, (2017), 10711-10716.